American Journal of Organic Chemistry 2026, 14(1): 1-9
DOI: 10.5923/j.ajoc.20261401.01

Synthesis, Comparison of Spectroscopic Properties and *In Silico* Analysis of Some Acyclic Derivatives of C5-Curcuminoids

Arjan Ganiji[1,2], Milena Kolevska[1], Jane Bogdanov[1,*]

[1]Institute of Chemistry, Faculty of Natural Sciences and Mathematics, Ss. Cyril and Methodius University, Arhimedova 5, 1000 Skopje, R. N. Macedonia
[2]Faculty of Technological Science, Mother Theresa University, Mirce Acev 4, 1000 Skopje, R. N. Macedonia

Abstract In this study six acyclic C5-curcuminoids containing different substituents on the aromatic rings were prepared by Claisen–Schmidt condensation and characterized by melting point measurements, FTIR and UV–Vis spectroscopy. Their physicochemical, pharmacokinetic and toxicological characteristics were further assessed using the SwissADME and ProTox-3.0 platforms. The FTIR spectra displayed the characteristic absorption of the conjugated carbonyl group in the 1650–1677 cm^{-1} range, whereas the UV–Vis absorption maxima occurred between 312 and 363 nm. These spectral variations suggest that aromatic substitution modifies the electronic environment of the conjugated dienone system. Among the synthesized compounds, Ib and Ic exhibited the most balanced SwissADME profiles, while the pronounced lipophilicity of Id represented its main unfavorable property. In comparison with curcumin, most of the C5 analogues were less polar and therefore showed different predicted membrane-permeation behavior. ProTox-3.0 identified a relatively limited number of toxicity alerts for most derivatives, although neurotoxicity and ecotoxicity were predicted for all six compounds. Taken together, the findings indicate that changes in aromatic substitution affect both the spectroscopic behavior and the predicted pharmacokinetic characteristics of C5-curcuminoids and support further experimental investigation of their biological and toxicological properties.

Keywords C5-curcuminoids, Synthesis, Spectroscopic properties, *in silico* analysis

1. Introduction

Curcumin (diferuloylmethane) is the principal bioactive constituent of turmeric, a dried powder obtained from the rhizomes of *Curcuma longa L*. It is one of the most extensively studied natural products due to its broad spectrum of therapeutic properties, including antioxidant, anticancer, antiprotozoal, antibacterial, anti-inflammatory, and neuroprotective activities [1].

Although curcumin exhibits remarkably low toxicity and promising anti-inflammatory and anticancer activities, both preclinical and clinical studies have demonstrated that its application in anticancer therapy is limited by its poor bioavailability and unfavorable pharmacokinetic profile, which result from its instability under physiological conditions [2]. For instance, in a Phase I clinical trial, oral administration of 3.6 g of curcumin daily resulted in only limited systemic exposure, with curcumin detected at low concentrations in plasma [3]. In a separate clinical study, following oral administration of 3.6 g of curcumin daily, curcumin concentrations in normal and malignant colorectal tissues were 12.7 ± 5.7 and 7.7 ± 1.8 nmol/g, respectively, while only trace levels were detected in the peripheral circulation [4]. Evidence from both in vitro and in vivo studies indicates that the β-diketone moiety is a major factor responsible for the instability and poor pharmacokinetic properties of curcumin [2]. Under in vitro conditions, curcumin is unstable at pH values above 6.5, which has been attributed to its chemical instability in aqueous media [2,5]. Furthermore, in vivo studies have shown that the β-diketone moiety serves as a substrate for enzymes of the aldo-keto reductase family, contributing to the rapid metabolism of curcumin in the body [6].

Over the past decade, considerable efforts have been dedicated to the synthesis of structurally modified curcumin derivatives aimed at enhancing their biological activities and improving their pharmacokinetic properties [2,7]. However, relatively few studies have focused specifically on improving the pharmacokinetic properties of curcumin [7]. It has been proposed that the stability and metabolic profile of curcumin can be enhanced by eliminating the β-diketone

* Corresponding author:
j_b_bogdanov@yahoo.com (Jane Bogdanov)
Received: Aug. 30; Accepted: Sep. 22, 2026; Published: Oct. 28, 2026
Published online at http://journal.sapub.org/ajoc

moiety [7]. Although earlier studies suggested that the β-diketone group was important for the biological activity of curcumin, more recent investigations have demonstrated that certain curcumin analogues containing a five-carbon enone bridge, but lacking the β-diketone moiety, retain or even exhibit enhanced inhibitory activity against the growth of various cancer cell lines [7,8]. These compounds are known as monocarbonyl analogs of curcumin (MACs) or C5-curcuminoids [7,8]. They possess the 1,5-diaryl-3-oxo-1,4-pentadienyl moiety, which represents an important structural pharmacophore, and exhibit diverse biological activities [8,9]. One proposed mechanism is that the electrophilic nature of these cross-conjugated dienones enables their reaction with biologically relevant thiols, including cysteine residues and glutathione, through Michael addition [9,10]. The aim of our work is to assess the solubility of C5-curcuminoids in organic solvents that are miscible with water for subsequent use to check their reactivity with biologically relevant thiols. It has been proposed that different aromatic substituents influence their activity and the reversibility of the *thi*a-Michael reaction. In addition, the synthesized compounds were evaluated using *in silico* approaches to assess their drug-likeness, predicted pharmacokinetic properties, and potential toxicological profiles.

The synthesized compounds were analyzed using the online platform SwissADME to evaluate their drug-likeness and to predict their molecular properties *in silico*. ADME (Absorption, Distribution, Metabolism, Excretion) modeling is a widely used computational approach for assessing the potential of a candidate compound to reach its biological target and exert its pharmacological effect.

2. Materials and Methods

The following reagents were used: acetone (Sigma-Aldrich), 2-bromobenzaldehyde (Aldrich), 2-methoxybenzaldehyde, 4-methoxybenzaldehyde (Merck), 2-fluorobenzaldehyde (Alfa Aesar), 2-(trifluoromethyl)-benzaldehyde (Sigma-Aldrich), 2,5-dimethylbenzaldehyde (Aldrich), methanol (Sigma-Aldrich), ethanol (Alkaloid), sodium hydroxide (Alkaloid), and dichloromethane (99.8% Fisher).

FTIR Spectroscopy

FTIR spectra were recorded using a ATR, Fourier-transform infrared (FTIR) spectrometer.

UV–Vis Spectroscopy

UV–Vis spectra were recorded on a Cary 50 UV–Vis spectrophotometer using a quartz cuvette. Acetonitrile or an appropriate mixture of acetonitrile and water (acetonitrile/ buffer) was used as the solvent.

***In Silico* ADME Prediction**

The synthesized compounds were analyzed using the online platform SwissADME to evaluate their drug-likeness and predict their molecular properties *in silico*. The radar plots generated by SwissADME provide a visual representation of the following physicochemical properties of the compounds: lipophilicity, molecular size, polarity, solubility, flexibility, and saturation. The ability of the compounds to permeate the blood–brain barrier (BBB) and their gastrointestinal (GI) absorption were predicted using the BOILED-Egg model.

***In Silico* Toxicity Prediction**

The toxicological properties of all synthesized compounds were predicted using the ProTox-3.0 platform. The analysis included the prediction of acute toxicity, hepatotoxicity, cytotoxicity, carcinogenicity, mutagenicity, and immunotoxicity.

General Procedure for the Synthesis of Acyclic C5-Curcuminoids

Acetone (7.5 mmol), the appropriate arylaldehyde (15 mmol), and methanol (10 mL) were placed in a 25 mL round-bottom flask. The reaction mixture was cooled in an ice bath and stirred for approximately 5 min. Afterwards, 2 mL of a 20% (w/v) aqueous sodium hydroxide solution was added dropwise over a period of 10 min. The reaction mixture was maintained in the ice bath with continuous stirring for an additional 20 min, after which the ice bath was removed, and stirring was continued at room temperature for a further 45 min. Distilled water (2 mL) was then added, and the reaction mixture was returned to the ice bath for another 10 min.

The resulting yellow suspension was collected by vacuum filtration through a Büchner funnel and washed successively with 10 mL of saturated ammonium chloride solution, distilled water (3 × 10 mL), and lastly with 5 mL of cold methanol. The resulting yellow precipitate was protected from direct light and dried for approximately 24 h. The crude products were purified by recrystallization from appropriate solvent(s) to afford yellow crystalline products.

Synthesis of (1*E*,4*E*)-1,5-bis(2-bromophenyl)penta-1, 4-dien-3-one (Ia, 2BrPhACE)

The crude product crystallized spontaneously upon evaporation of methanol to afford yellow crystals (84% yield); mp 66–68 ℃ (lit. 64–66 ℃, [10,11]); UV–Vis (80:20 CH_3CN/H_2O): λ_max = 318, 237.9, and 207.9 nm. FTIR (ATR, ν, cm^{-1}): 3015 (Ar–C–H), 1605 (C=O), 1480–1460 (Ar C=C), 697 (C–Br). R_f (hexane/ethyl acetate, 8:1) = 0.30.

Synthesis of (1*E*,4*E*)-1,5-bis(2-methoxyphenyl)penta-1, 4-dien-3-one (Ib, 2OMePhACE)

Recrystallized from methanol to afford yellow crystals (96% yield); mp 124–125 ℃ (lit. 111–114 ℃, [12]); UV–Vis (80:20 CH_3CN/H_2O): λ_{max} = 363 and 212 nm. FTIR (ATR, ν, cm^{-1}): 3030 (Ar–C–H), 1612 (C=O), 1485–1435 (Ar C=C). R_f (hexane/ethyl acetate, 8:1) = 0.12.

Synthesis of (1*E*,4*E*)-1,5-bis(4-methoxyphenyl)penta-1, 4-dien-3-one (1c, 4OMePhACE)

Recrystallized from methanol to afford yellow crystals (93% yield); mp 125–126 ℃ (lit. 121–122 ℃, [12]); UV–Vis (80:20 CH_3CN/H_2O): λ_{max} = 357.9 and 239 nm. FTIR (ATR, ν, cm^{-1}): 3009 (Ar–C–H), 1628 (C=O), 1593–1571 (Ar C=C). R_f (hexane/ethyl acetate, 8:1) = 0.08.

Synthesis of (1*E*,4*E*)-1,5-bis[2-(trifluoromethyl)phenyl] penta-1,4-dien-3-one (1d, 2CF_3PhACE))

Recrystallized from methanol to afford yellow crystals (82% yield); mp 126–128 ℃ (lit. 131 ℃, [2]). UV–Vis (80:20 CH_3CN/H_2O): λ_{max} = 312 and 227 nm. FTIR (ATR, ν,

cm^{-1}): 3100 (Ar–C–H), 1677 (C=O), 1631–1572 (Ar C=C), 1278 (Ar–C–F). R_f (hexane/ethyl acetate, 8:1) = 0.15.

Synthesis of (1*E*,4*E*)-1,5-bis(2,5-dimethylphenyl)penta-1,4-dien-3-one (1e)

Recrystallized from a CH_2Cl_2/CH_3OH (1:1, v/v) mixture to afford yellow crystals (91 % yield); mp 138–139 ℃ (lit. 140–142 ℃, [2]); UV–Vis (80:20 CH_3CN/H_2O): λ_{max} = 337.1 and 210.9 nm. FTIR (ATR, ν, cm^{-1}): 3050 (Ar–C–H), 1662 (C=O), 1619–1578 (Ar C=C). R_f (hexane/ethyl acetate, 8:1) = 0.41.

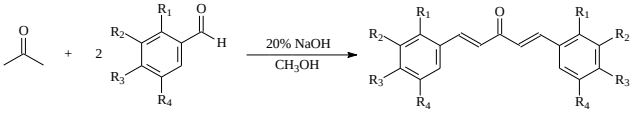
Synthesis of (1*E*,4*E*)-1,5-diphenylpenta-1,4-dien-3-one (I-H, H-PhACE)

Recrystallized from ethyl acetate to afford yellow crystals (68% yield); mp 110–111 ℃ (lit. 110–112 ℃, [10]). UV–Vis (80:20 CH_3CN/H_2O): λ_{max} = 326 and 228 nm. FTIR (ATR, ν, cm^{-1}): 3050 (Ar–C–H), 1650 (C=O), 1593–1571 (Ar C=C). R_f (hexane/ethyl acetate, 8:1) = 0.70.

3. Results and Discussion

Synthesis and Characterization

The synthesis of the 1,5-bisphenylpenta-1,4-dien-3-one derivatives was carried out using a modified procedure based on the method reported by [13]. The synthesized compounds were obtained via the Claisen–Schmidt condensation, a specific type of aldol condensation that proceeds between an aromatic aldehyde and acetone. The reaction was catalyzed under basic conditions using sodium hydroxide (NaOH).



Ia : R_1 = Br ; R_2 = H ; R_3 = H ; R_4 = H
Ib : R_1 = OCH_3 ; R_2 = H ; R_3 = H ; R_4 = H
Ic : R_1 = H ; R_2 = H ; R_3 = OCH_3 ; R_4 =H
Id : R_1 = CF_3 ; R_2 = H ; R_3 = H ; R_4 = H
Ie : R_1 = CH_3 ; R_2 = H ; R_3 = H ; R_4 = CH_3
I-H : R_1 = H; R_2 = H ; R_3 = H ; R_4 = H

Figure 1. Synthesis of C5-curcuminoids:
Ia, (1*E*,4*E*)-1,5-bis(2-bromophenyl)penta-1,4-dien-3-one;
Ib, (1*E*,4*E*)-1,5-bis(2-methoxyphenyl)penta-1,4-dien-3-one;
Ic, (1*E*,4*E*)-1,5-bis(4-methoxyphenyl)penta-1,4-dien-3-one;
Id, (1*E*,4*E*)-1,5-bis[2-(trifluoromethyl)phenyl]penta-1,4-dien-3-one;
Ie, (1*E*,4*E*)-1,5-bis(2,5-dimethylphenyl)penta-1,4-dien-3-one

Table 1. Melting points, spectroscopic, and chromatographic data of the synthesized compounds

Compound	T_m (℃)	FT-IR-ATR cm^{-1}	UV-VIS $\lambda_{max\ 1}$ (80/20 CH_3CN : H_2O)	UV-VIS $\lambda_{max\ 2}$ (80/20 CH_3CN : H_2O)	TLC, R_f
Ia (2BrPhACE)	66-68	1671 (C = O)	322 nm	238 nm	0.30
Ib (2OMePhACE)	124-125	1668 (C = O)	363 nm	212 nm	0.12
Ic (4OMePhACE)	125-126	1655 (C = O)	358 nm	239 nm	0.10
Id ($2CF_3$PhACE)	126-128	1677 (C = O)	312 nm	227 nm	0.15
Ie (2,5DiMePhACE)	138-139	1662 (C = O)	337 nm	210,9 nm	0.41
I-H (1HPhACE)	110-111	1650 (C = O)	326 nm	228 nm	0.70

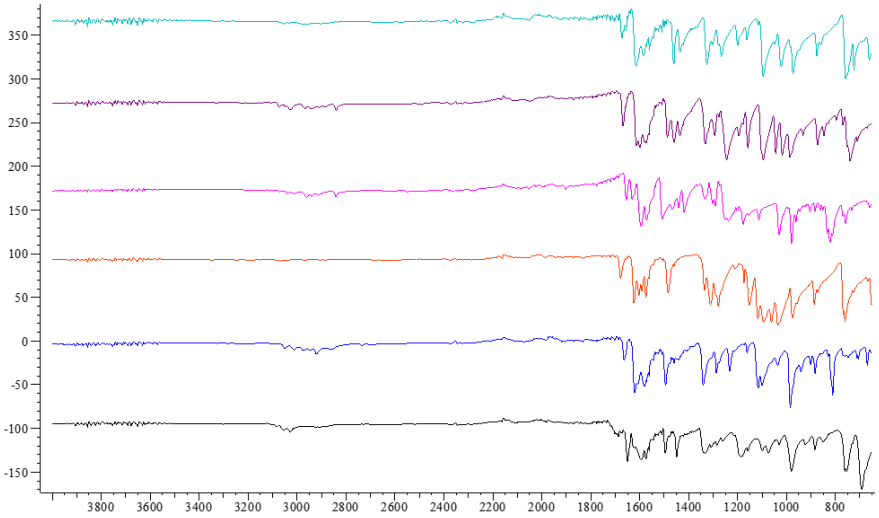


Figure 2. FT-IR-ATR spectra of the synthesized compounds: **Ia** (turquoise); **Ib** (purple); **Ic** (magenta); **Id** (orange); **Ie** (blue); **I-H** (black)

All synthesized compounds exhibited a characteristic absorption band within the range of 1650-1677 cm^{-1}, which was assigned to the stretching vibration of the conjugated carbonyl group (C=O). Aromatic compounds showed a weak absorption band in the region of 3010-3100 cm^{-1}, corresponding to the stretching vibrations of -CH bonds. The absorption bands observed in the region of 2970-2830 cm^{-1} are attributed to C-H stretching vibrations of bonds involving carbon atoms with sp^3 hybridization. Aromatic compounds displayed a series of medium-intensity absorption bands in the region of 1450-1600 cm^{-1}, associated with aromatic C=C stretching vibrations. Aryl and alkyl halides exhibited characteristic absorption bands in the region of 500-800 cm^{-1} [14]. The observed differences in the C=O stretching frequencies are relatively small but indicate that the nature of the substituents influences the electronic environment of the carbonyl group [15]. Compared with the unsubstituted compound I-H, the substituted derivatives showed an increase of 5–27 cm^{-1} in the C=O stretching frequency, with the largest difference observed for the CF_3 derivative Id. The UV–Vis absorption maxima also varied with the type and position of the aromatic substituents, showing shifts toward either longer or shorter wavelengths. The unsubstituted derivative (**I-H**) displayed the lowest value (1650 cm^{-1}) for the C=O band reflecting the effective conjugation of the carbonyl group with the α,β-unsaturated system and the two phenyl rings [15,16]. The introduction of electron-withdrawing substituents, particularly the $-CF_3$ group, resulted in a shift of the C=O band toward higher wavenumbers, consistent with a reduced contribution of conjugative electron delocalization and increased effective double-bond character of the carbonyl group [15,17]. In contrast, electron-donating substituents ($–OCH_3$ and $–CH_3$) produced smaller changes in the C=O stretching frequency, particularly in the para-methoxy derivative Ic. These groups can modify the electron distribution within the conjugated system through resonance and inductive effects, while the carbonyl stretching frequency is also influenced by the local electronic environment and molecular conformation. Therefore, the FT-IR analysis demonstrates that the electronic effects of the substituents induce subtle changes in the strength of the C=O bond while preserving the characteristic unsaturated carbonyl framework of the synthesized derivatives.

These prepared C5-curcuminoids were checked for their solubility in organic solvents that are miscible with water (methanol, 95% ethanol and acetonitrile). Their solubility was the highest in acetonitrile and mixtures up to 20% (v/v) with water could be prepared, which were suitable for UV-Vis spectroscopic measurements. The UV-Vis spectra of the synthesized derivatives exhibited pronounced differences in their absorption maxima (312-363 nm), reflecting the influence of the electronic nature of the substituents on the extent of π-conjugation [15,16]. Electron-donating substituents, particularly the methoxy group, induced bathochromic shifts, whereas the strongly electron-withdrawing $-CF_3$ substituent caused a hypsochromic shift relative to the unsubstituted derivative [15,16]. These spectral variations indicate that the electronic structure of the conjugated enone system can be effectively tuned by appropriate substitution [15,16]. Since the α,β-unsaturated carbonyl moiety is the reactive site toward *thia*-Michael addition, the observed absorption bands in the near-UV region are expected to change upon disruption of the conjugated system during the reaction [9,18]. Therefore, these compounds are suitable candidates for monitoring thiol addition kinetics by UV-Vis spectroscopy by following the decrease or shift of the characteristic absorption band over time [9,18].

***In Silico* ADME Analysis**

The BOILED-Egg model was applied to provide a preliminary assessment of the absorption and distribution characteristics of the synthesized compounds. This model uses lipophilicity (WLOGP) and topological polar surface area (TPSA) to estimate the probability of passive gastrointestinal absorption and penetration through the blood–brain barrier (BBB) [19,20]. Compounds **Ib**, **Ic** and **I-H** are situated within the yellow region of the diagram, indicating physicochemical properties favorable for gastrointestinal uptake and potential passage across the blood-brain barrier. This predicted behavior is most likely associated with their comparatively low TPSA values and moderate lipophilicity.

A somewhat different pattern was observed for compounds **Ia** and **Ie**. These derivatives possess higher WLOGP values and are positioned close to the upper boundary of the region associated with BBB penetration. Although both compounds retain relatively low polarity, their increased lipophilicity may reduce their predicted ability to cross the blood–brain barrier compared with **Ib**, **Ic** and **I-H**.

Compound **Id** showed the most pronounced deviation from the other derivatives. The presence of two trifluoromethyl groups substantially increases its calculated lipophilicity, placing this compound outside the prediction range of the BOILED-Egg model. This observation suggests that excessive lipophilicity may adversely affect its predicted absorption and distribution profile, despite its relatively low polar surface area.

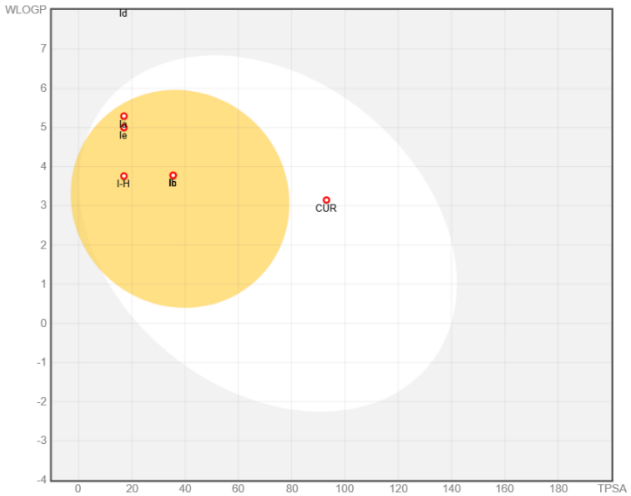


Figure 3. BOILED-Egg plot of the synthesized compounds (Ib and Ic are overlapped)

Another relevant observation is that all investigated compounds were classified as P-glycoprotein non-substrates (PGP-). The SwissADME platform includes P-gp substrate prediction together with other pharmacokinetic and drug-likeness parameters [19]. Consequently, P-gp-mediated efflux is not expected to exert a major influence on the transport of these compounds. Overall, the BOILED-Egg predictions indicate that substitution of the aromatic rings noticeably influences the expected pharmacokinetic behavior of the investigated C5-curcuminoids. Among the derivatives studied, **Ib**, **Ic** and **I-H** appear to possess the most suitable balance between polarity and lipophilicity, whereas the markedly higher lipophilicity of Id seems to be the principal factor responsible for its less favorable position in the model [19].

Curcumin (**CUR**), included as a reference compound, showed a different position in the BOILED-Egg plot compared with several of the synthesized C5-curcuminoids. CUR is located within the white region, but outside the yellow yolk, indicating a favorable probability of passive gastrointestinal absorption, while penetration across the blood-brain barrier is not predicted. Its position can mainly be attributed to its considerably higher topological polar surface area (TPSA) compared with most of the synthesized derivatives. The greater polarity of curcumin limits its predicted BBB permeability despite its moderate lipophilicity. In contrast, compounds **Ib**, **Ic** and **I-H**, which possess lower TPSA values, are positioned within the yellow region and are therefore predicted to have a higher probability of crossing the blood-brain barrier (BBB). This comparison suggests that removal of the β-diketone-containing curcumin framework and modification of the aromatic substituents in the C5-curcuminoids considerably alter the balance between polarity and lipophilicity, which in turn affects their predicted distribution properties.

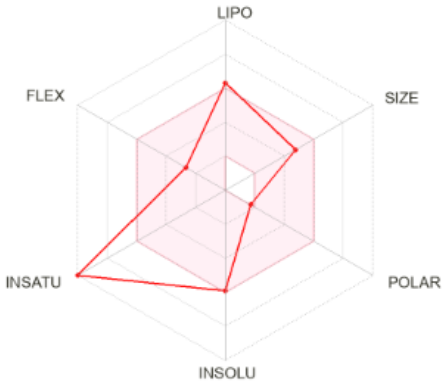
The bioavailability radar plots compare the main physicochemical properties of the synthesized C5-curcuminoids and curcumin (CUR), including lipophilicity, molecular size, polarity, solubility, saturation and flexibility [20].

Among the synthesized compounds, **Ib** and **Ic** show the most balanced profiles. Both have identical molecular weights, TPSA values and WLOGP values, and their methoxy groups increase polarity while maintaining moderate lipophilicity. The similarity of their radar plots suggests that changing the methoxy group from the ortho to the para position has only a limited effect on the overall physicochemical descriptors considered by SwissADME.

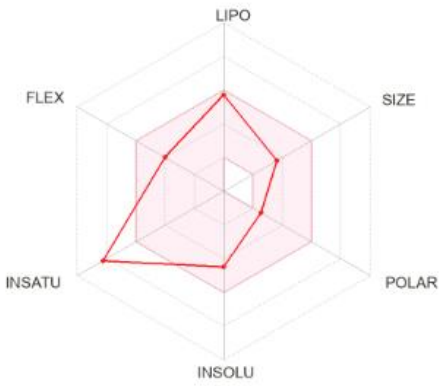
The unsubstituted derivative **I-H** also shows a generally favorable profile, with low molecular weight and moderate lipophilicity, although its low TPSA reflects reduced polarity. In contrast, **Ia** and **Ie** are more lipophilic, while their polarity remains low. The most pronounced deviation is observed for **Id**, where the two trifluoromethyl groups markedly increase lipophilicity, resulting in a WLOGP value of 8.11. This agrees with the BOILED-Egg analysis, where Id also showed the least favorable position.

A common feature of the C5-curcuminoids is their relatively low saturation, which can be related to the high proportion of sp^2-hybridized carbon atoms in the aromatic rings and conjugated dienone system. This should therefore be considered mainly as a structural feature of the C5-curcuminoid scaffold.

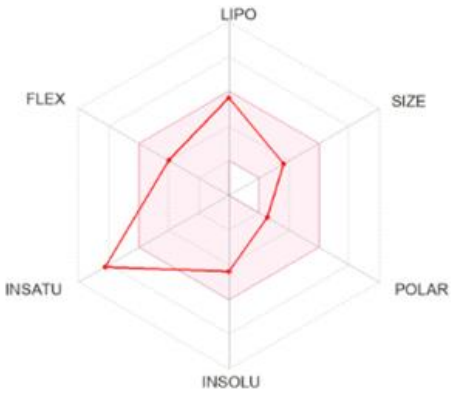
The radar profile of curcumin differs from those of most C5 analogues. Its WLOGP value is moderate, while its TPSA is considerably higher due to the presence of several oxygen-containing groups. Thus, curcumin is more polar than most of the synthesized derivatives. However, its apparently favorable radar profile should not be interpreted as direct evidence of good experimental bioavailability, since its pharmacokinetic behavior is also influenced by chemical instability, metabolism and tautomerism.



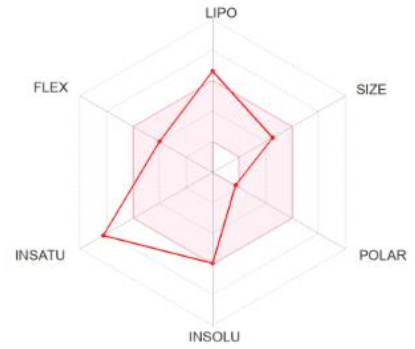
1a



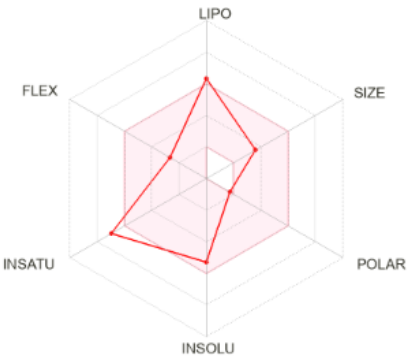
1b



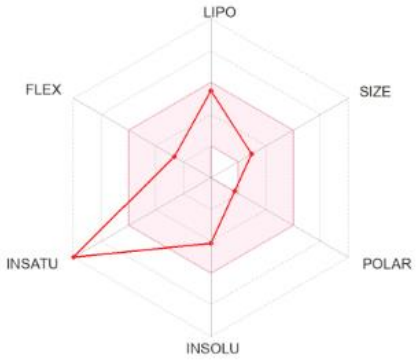
1c



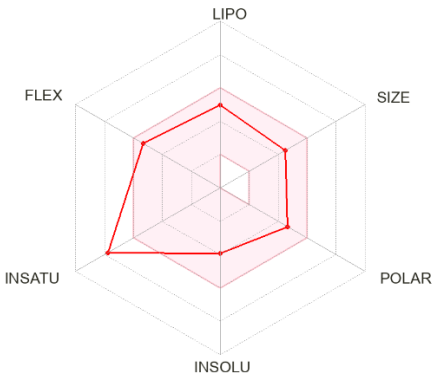
1d



1e



I-H



CUR

Figure 4. Bioavailability radar plots generated by SwissADME for the synthesized compounds

Overall, **Ib** and **Ic** display the most favorable balance between polarity and lipophilicity, whereas **Id** is distinguished by excessive lipophilicity. Despite these differences, all investigated compounds, including curcumin, have the same predicted bioavailability score of 0.55, showing that the radar plots provide useful additional information about the individual physicochemical factors influencing each compound.

Molecular properties, including the partition coefficient, molecular weight, hydrogen bond donors and acceptors, topological polar surface area (TPSA), as well as the violations of Lipinski's rule of five, were evaluated and are presented in Table 2.

Topological polar surface area (TPSA) is an important pharmacokinetic parameter widely used in drug development for predicting the ADME properties of potential drug candidates. This parameter reflects the polar surface area of a molecule and plays a significant role in its interactions with biological targets, as well as in its ability to permeate biological membranes. According to the data presented in Table 2, all analyzed compounds exhibited TPSA values within the range considered favorable for good potential oral bioavailability.

Table 2. Predicted physicochemical properties, drug-likeness parameters, and bioavailability-related properties of the synthesized compounds using SwissADME

Comp.	MW	HBA	HBD	TPSA	WLOGP	Lipinski ROF	Synthetic accessibility	Bioavailability score
Ia	392	1	0	17.07	5.29	1	2.7	0.55
Ib	294	3	0	35.53	3.78	0	2.77	0.55
Ic	294	3	0	35.53	3.78	0	2.52	0.55
Id	370	7	0	17.07	8.11	1	2.96	0.55
Ie	290	1	0	17.07	5.00	1	3.06	0.55
I-H	234	1	0	17.07	3.76	0	2.45	0.55
CUR	368	6	2	93.06	3.15	0	2.97	0.55

According to Lipinski's Rule of Five, which is a widely accepted criterion in drug discovery and development for evaluating drug-like properties, an orally active drug candidate should not violate more than one of the established criteria. As shown in Table 2, all investigated compounds complied with these requirements, with exception of more lipophilic compounds **Ia**, **Id** and **Ic** which have MLOGP> 4.15.

***In Silico* Toxicological Analysis**

The potential toxicological characteristics of the synthesized C5-curcuminoids were assessed using the ProTox-3.0 platform [21]. The predicted toxicological properties of the synthesized compounds and curcumin (CIR) are presented in Table 3. ProTox-3.0 is an *in silico* toxicity prediction tool based on molecular similarity and machine-learning approaches, allowing the estimation of a broad range of toxicological endpoints [21]. Hepatotoxicity, respiratory toxicity, immunotoxicity, mutagenicity, cytotoxicity, clinical toxicity and nutritional toxicity were classified as inactive for all synthesized derivatives. Within the limitations of the computational approach, these findings suggest the absence of major alerts for these particular toxicity endpoints.

In contrast, neurotoxicity and ecotoxicity were predicted as active for all six C5-curcuminoids. Since this tendency was observed throughout the series despite differences in aromatic substitution, it may be related to structural features common to the C5-curcuminoid scaffold. Nevertheless, this assumption remains speculative and requires experimental confirmation.

Certain compound-specific variations were also observed. Compound **Ia** was predicted to show cardiotoxic and carcinogenic potential, while these endpoints were classified as inactive for the other synthesized analogues. The additional toxicity alerts observed for **Ia** could be associated with the ortho-bromine substituents on the aromatic rings, which may alter its physicochemical characteristics and interactions with biological targets. Nevertheless, the available computational data do not allow a definite link to be established between bromine substitution and the predicted toxic effects. Compound **Ic** showed an additional alert for nephrotoxicity. Accordingly, **Ib**, **Id**, **Ie** and **I-H** showed fewer predicted toxicity alerts than **Ia** and **Ic**, although this finding alone is insufficient to establish a more favorable overall safety profile.

The predicted toxicity profiles of the synthesized C5-curcuminoids differed from that of curcumin (CUR). In contrast to CUR, which was classified as inactive for neurotoxicity and ecotoxicity, all six derivatives showed positive predictions for these endpoints. Curcumin, however, exhibited additional alerts for nephrotoxicity, cardiotoxicity, immunotoxicity and clinical toxicity. Among the synthesized compounds, **Ib**, **Id**, **Ie** and **I-H** presented the lowest number of predicted toxicity alerts, whereas **Ia** and **Ic** displayed additional potential toxic effects. These variations suggest that changes in molecular structure may affect the predicted toxicological behavior of the investigated.

Taken together, the ProTox-3.0 results revealed a relatively restricted number of predicted toxicity alerts for most of the investigated derivatives, with neurotoxicity and ecotoxicity representing the common findings across the entire series. These outcomes should, however, be interpreted as preliminary computational estimates rather than experimentally established toxic effects. Additional biological and toxicological investigations are therefore necessary to determine the actual safety profiles of these C5-curcuminoids. The predicted toxicological properties of the synthesized compounds are presented in Table 3.

4. Conclusions

Six acyclic C5-curcuminoids with different aromatic substituents were synthesized by Claisen–Schmidt condensation and characterized by FTIR and UV–Vis spectroscopy. The spectral differences confirmed that the substituents influence the electronic properties of the conjugated dienone system.

Table 3. ProTox-3.0 [21] predictions of toxicological properties for six synthesized C5-curcuminoids (Ia–Ie, I-H) and curcumin (CUR)

Target	Ia	Ib	Ic	Id	Ie	I-H	CUR
Hepato-toxicity	inact*	inact	inact	inact	inact	inact	inact
Neuro toxicity	act**	act	act	act	act	act	inact
Nephro toxicity	inact	inact	act	inact	inact	inact	act
Respirat. toxicity	inact	inact	inact	inact	inact	inact	inact
Cardio toxicity	act	inact	inact	inact	inact	inact	act
Carcinogenicity	act	inact	inact	inact	inact	inact	inact
Immuno toxicity	inact	inact	inact	inact	inact	inact	act
Mutagenicity	inact	inact	inact	inact	inact	inact	inact
Cyto-toxicity	inact	inact	inact	inact	inact	inact	inact
Eco-toxicity	act	act	act	act	act	act	inact
Clinical toxicity	inact	inact	inact	inact	inact	inact	act
Nutritio- nal toxicity	inact	inact	inact	inact	inact	inact	inact

act ** (active): the model predicts a potential toxicity alert for the specified endpoint; inact* (inactive): no toxicity alert is predicted for that endpoint. These are computationally derived based on molecular similarity and machine-learning models.

SwissADME analysis showed that **Ib** and **Ic** had the most balanced physicochemical profiles, while **I-H** also displayed favorable predicted properties. In contrast, the high lipophilicity of **Id** was its main limitation. Compared with curcumin, most C5 analogues were less polar, which affected their predicted membrane permeability and distribution.

ProTox-3.0 indicated relatively few toxicity alerts for most compounds, although neurotoxicity and ecotoxicity were predicted for all derivatives, with additional alerts for **Ia** and **Ic**. These findings require experimental confirmation.

Overall, the results show that aromatic substitution can modify both the spectroscopic and predicted pharmacokinetic properties of C5-curcuminoids. The synthesized compounds therefore represent a useful series for further studies of thiol reactivity, biological activity and toxicity. in silico toxicity assessment revealed a low predicted toxicological risk, suggesting that the synthesized C5 curcuminoid derivatives represent promising candidates for further biological evaluation.

REFERENCES

[1] Ardiansah B., Hardhani M. R., Putera D., Wukirsari T., Cahyana A. H., Jia J., Khan M., Design, synthesis, and antioxidant evaluation of monocarbonyl curcumin analogues tethered 1,2,3-triazole scaffold, *Case Studies in Chemical and Environmental Engineering* 8 (2023) 100425.

[2] Liang G., Shao L., Wang Y., Zhao Ch., Chu Y., Xiao J., Zhao Y., Li X., Yang Sh., Exploration and synthesis of curcumin analogues with improved structural stability both in vitro and in vivo as cytotoxic agents, *Bioorganic and Medicinal Chemistry* 17 (2009) 2623-2631.

[3] Sharma R. A., Euden S. A., Platton S. L., Cooke D. N., Shafayat A., Hewitt H. R., Marczylo T. H., Morgan B., Hemingway D., Plummer S. M., Pirmohamed M., Gescher A. J., Steward W. P., Phase I clinical trial of oral curcumin: biomarkers of systemic activity and compliance, *Clinical Cancer Research* 10 6847-6854 (2004).

[4] Garcea G., Berry D. P., Jones D. J. L., Singh R., Dennison A. R., Farmer P. B., Sharma R. A., Steward W. P., Gescher A. J., Consumption of the putative chemopreventive agent curcumin by cancer patients: assessment of curcumin levels in the colorectum and their pharmacodynamic consequences, *Cancer Epidemiology, Biomarkers and Prevention* 14 (2005) 120–125.

[5] Kharat M., Du Z., Zhang G., McClements D. J., Physical and Chemical Stability of Curcumin in Aqueous Solutions and Emulsions: Impact of pH, Temperature, and Molecular Environment, *Journal of Agricultural and Food Chemistry* 65 (2017) 1525–1532.

[6] Kumar A., et al., Structure based comprehensive modelling, spatial fingerprints mapping and ADME screening of curcumin analogues as novel ALR2 inhibitors, *Journal of Molecular Graphics and Modelling* 70 (2017) 208–221.

[7] Vieira T. M., Tanajura L. S., Heleno V. C. G., Magalh ães L. G., Crotti A. E. M., Monoketone Curcuminoids: An Updated Review of Their Synthesis and Biological Activities, *Future Pharmacology* 4 (2024) 54-76.

[8] Yamakoshi H., Ohori H., Kudo C., Sato A., Kanoh N., Ishioka C., Shibata H., Iwabuchi Y., Structure–activity relationship of C5-curcuminoids and synthesis of their molecular probes thereof, *Bioorganic and Medicinal Chemistry* 18 (2010) 1083-1092.

[9] Lozanovski Z., Petreska Stanoeva J., Bogdanov J., Development of a spectrophotometric method for assessment of the relative reactivity of monocarbonyl analogs of curcumin with 2-(dimethylamino)ethanethiol, *Macedonian Journal of Chemistry and Chemical Engineering* 42 (2023) 13–24.

[10] Clariano L. M., et al., Monocarbonyl Analogs of Curcumin with Potential to Treat Colorectal Cancer, *Chemistry and Biodiversity* 20 (2023) e202300222.

[11] Xiao J., Tan Y., Pan Y., Liang G., Qu Ch., Zhang X., Zhang Y., Li X., Yang H., A new cyclooxygenase-2 inhibitor (1E,4E)-1,5-Bis(2-bromophenyl)penta-1,4-dien-3-one (GL63) suppresses cycloogenase-2 gene expression in human lung epithelial cancer cells: Coupled mRNA stabilization and posttranscriptional inhibition, *Biol Pharm Bull* 33(7) 1170-1175 (2010).

[12] Zamrus S.N.H., Akhtar M.N., Yeap S.K., Quah Ch. K., Loh W., Alitheen N.B., Zareen S., Tajuddin S. N., Hussin Y., Shah S.A.A., Design, synthesis and cytotoxic effects of curcuminoids on HeLa, K562, MCF-7 and MDA-MB-231 cancer cell lines, *Chemistry Central Journal* (2018) 12:31.

[13] Qiu Ch., Hu Y., Wu K., Yang K., Wang N., Ma Y., Zhu H., Zhang Y., Zhao Y., Chen Ch., Li Sh., Fu L., Synthesis and biological evaluation of allylated mono-carbonyl analogues of curcumin (MACs) as anti-cancer agents for cholangiocarcinoma, *Bioorganic and Medicinal Chemistry Letters* 2016, 26: 5971-5976.

[14] Nandiyanto A., Oktiani R., Ragadhita R., How to Read and Interpret FTIR Spectroscope of Organic Material, *Indonesian Journal of Science and Technology* (2019), 4(1): 97.

[15] Silverstein R. M., Webster F. X., Kiemle D. J., Bryce D. L., Spectrometric Identification of Organic Compounds, 8th ed., John Wiley and Sons, New York, 2014.

[16] Yamakoshi H., Ohori H., Kudo C., Sato A., Kanoh N., Ishioka C., Shibata H., Iwabuchi Y., Structure–activity relationship of C5-curcuminoids and synthesis of their molecular probes thereof, *Bioorganic and Medicinal Chemistry* 18 (2010) 1083-1092.

[17] Vatsadze S. Z., Golikov A. G., Kriven'ko A. P., Zyk N. V., Chemistry of Cross-Conjugated Dienones, Russian Chemical Reviews, 77 (8) (2008) 661-681.

[18] Witzke A. A., et al., Covalent Modifiers: A Chemical Perspective on the Reactivity of α,β-Unsaturated Carbonyls with Thiols via Hetero-Michael Addition Reactions, *Chemical Research in Toxicology* 30 (2017) 1-17.

[19] Daina, A., Zoete, V,. A BOILED-Egg to predict gastrointestinal absorption and brain penetration of small molecules. *ChemMedChem*, 11(11) (2016) 1117–1121.

[20] Daina, A., Michielin, O., Zoete, V. (2017). SwissADME: A free web tool to evaluate pharmacokinetics, drug-likeness and medicinal chemistry friendliness of small molecules. *Scientific Reports*, 7, 42717.

[21] Banerjee P., Kemmler E., Dunkel M., Preissner R., ProTox 3.0: a webserver for the prediction of toxicity of chemicals, *Nucleic Acids Research* 52 (2024) W513–W520.

Copyright © 2026 The Author(s). Published by Scientific & Academic Publishing
This work is licensed under the Creative Commons Attribution International License (CC BY). http://creativecommons.org/licenses/by/4.0/